Preprints of the 18th IFAC World Congress
Milano (Italy) August 28 - September 2, 2011

Position and Velocity USBL/IMU Sensor-based Navigation Filter ⋆

M. Morgado, P. Batista, P. Oliveira, and C. Silvestre

Institute for Systems and Robotics, Instituto Superior Técnico
Av. Rovisco Pais, 1, 1049-001, Lisbon, Portugal
{*marcomorgado,pbatista,pjcro,cjs*}*@isr.ist.utl.pt*

Abstract: This paper presents a novel approach to the design of globally asymptotically stable (GAS) position and velocity filters for Autonomous Underwater Vehicles (AUVs) based directly on the nonlinear sensor readings of an Ultra-short Baseline (USBL) acoustic system and two triads of accelerometers and angular rate gyros, from an Inertial Measurement Unit (IMU). The devised solution has its foundation on the derivation of a linear time-varying (LTV) system that is shown to mimic the dynamical behavior of the original nonlinear system, and allows for the use of powerful linear system analysis and filtering design tools, yielding GAS filter error dynamics. Simulation results reveal that the proposed filter is able to achieve the same level of performance of more traditional solutions, such as the Extended Kalman Filter (EKF), while providing, at the same time, GAS guarantees which are absent for the EKF.

Keywords: Marine system navigation, guidance and control; autonomous underwater vehicles; Kalman filtering techniques in marine systems control; nonlinear observer and filter design.

1. INTRODUCTION

Among several critical and key steps towards the successful operation of autonomous vehicles, the design and implementation of navigation systems certainly plays a major role on the capability of such vehicles to perform precision-demanding tasks. An interesting and detailed survey on underwater vehicle navigation and its relevance can be seen in Whitcomb [2000]. Acoustic based positioning devices step forward as the primordial choice for accurate underwater navigation. As opposed to have only one on-board acoustic receiver and a set of floating or moored acoustic transponders, an Ultra-Short Baseline (USBL) underwater positioning device is composed of a small calibrated array of acoustic receivers installed on-board the Underwater Vehicle (UV). This paper presents an approach to the design of globally asymptotically stable (GAS) position and velocity filters directly based on the nonlinear range array sensor readings and inertial motion measurements.

In the considered mission scenarios an underwater vehicle is equipped with an USBL underwater positioning device, and an Inertial Measurement Unit (IMU), that consists of a triad of orthogonally mounted rate gyros and a triad of orthogonally mounted accelerometers, and operates in the vicinity of a fixed transponder, as depicted in Fig. 1. Given the proximity of the sensors in the receiving array, hence the name Ultra-Short Baseline (USBL), the USBL is capable of measuring more accurately the Range-Difference-of-Arrival (RDOA) of the acoustic waves at the receivers compared to the actual distances between the transponder and all the receivers installed on-board. To reduce the impact of noisy measurements, the uncertainty on the local gravity vector estimate, and the nonlinear nature of the range measurements, a filtering solution is required in order to correctly estimate the position of the transponder in the vehicle coordinate frame and the inertial velocity of the vehicle.

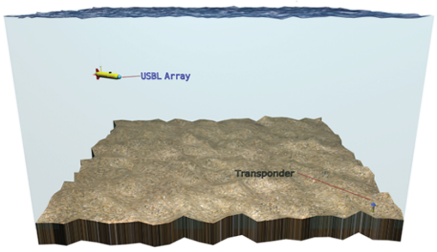

Fig. 1. Mission scenario

Recent advances in the area of underwater navigation based on merging the information from acoustic arrays and other inertial sensors, can be found in Rigby et al. [2006], Willemenot et al. [2009], Batista et al. [2010] and references therein. Classical filtering strategies often resort to the well known Extended Kalman Filter (EKF), see Morgado et al. [2006a], Particle Filters (PF), see Rigby et al. [2006], which lack global asymptotic stability properties, or to filtering solutions that use a precomputed position fix from the USBL device using the range and bearing and elevation angles of the transponder. The computation of this position fix often resorts to a Planar-Wave approximation of the acoustic wave arriving at the receiving array, previously used by the authors in Morgado

⋆ This work was supported by FCT (ISR/IST plurianual funding) through the PIDDAC Program funds, by the project FCT PTDC/EEA-CRO/111197/2009 - MAST/AM of the FCT, and by the EU Project TRIDENT (Contract No. 248497). The work of Marco Morgado was supported by PhD Student Scholarship SFRH/BD/25368/2005 from the Portuguese FCT POCTI programme.

et al. [2006a]. The usage of this approximation undermines (see Morgado et al. [2006b]) the convergence guarantees for such traditional designs, which is a desirable feature if the vehicle is to dock to a station or manoeuvre in the vicinity of a transponder.

The main contribution of this paper lies on the design of a globally asymptotically stable sensor-based filter to estimate the position of the transponder in the vehicle frame, the vehicle velocity in body-fixed coordinates, whilst explicitly estimating the unknown local gravity vector present in the accelerometers specific force readings. The solution presented in the paper departs from previous approaches as the range measurements are directly embedded in the filter structure, thus avoiding the planar-wave approximation, and extends the framework presented in Morgado et al. [2010], where a Doppler Velocity Log (DVL) that measures the fluid relative velocity was considered instead of an IMU. The DVL has the disadvantage of being an active-acoustic device, as opposed to the passive nature of the accelerometer readings. The framework presented herein also follows related work found in Batista et al. [2009], where single range measurements were considered and persistent excitation conditions were imposed on the vehicle motion to bear the system observable. In this paper the framework is extended to the case of having an array of receivers installed on-board the vehicle, which allows for the analysis of the overall system without any restriction on the vehicle motion.

The paper is organized as follows: Section 2 sets the problem framework and definitions. The proposed filter design and main contributions of the paper are presented in Section 3 where the filter structure is brought to full detail and an extensive observability analysis is carried out. Due to space limitations, only brief guidelines on the theorem proofs are provided, and the full proofs are reserved for a further extended version of this work. Simulation results and performance comparison with traditional solutions are discussed in Section 4, and finally Section 5 provides some concluding remarks.

2. PROBLEM FRAMEWORK

In order to set the design framework, let $\{I\}$ denote an inertial reference coordinate frame and $\{B\}$ a coordinate frame attached to the vehicle, usually denominated as body-fixed coordinate frame. The position of the transponder $\mathbf{r}(t) \in \mathbb{R}^3$ in the vehicle coordinate frame $\{B\}$ is given by

$$\mathbf{r}(t) = \mathcal{R}^T(t)(\mathbf{s} - \mathbf{p}(t)), \tag{1}$$

where $\mathbf{s} \in \mathbb{R}^3$ is the position of the transponder in inertial coordinates, $\mathbf{p}(t) \in \mathbb{R}^3$ is the position of the vehicle in inertial coordinates, and $\mathcal{R}(t) \in SO(3)$ is the rotation matrix from $\{B\}$ to $\{I\}$. The time derivative of $\mathcal{R}(t)$ verifies $\dot{\mathcal{R}}(t) = \mathcal{R}(t)\mathcal{S}(\omega(t))$, where $\omega(t) \in \mathbb{R}^3$ is the angular velocity of $\{B\}$ with respect to $\{I\}$, expressed in body-fixed coordinates, and $\mathcal{S}(\omega(t))$ is the skew-symmetric matrix that represents the cross product, i.e., $\mathcal{S}(\omega)\, a = \omega \times a$.

Time differentiation of (1) yields

$$\dot{\mathbf{r}}(t) = -\mathcal{S}(\omega(t))\,\mathbf{r}(t) - \mathbf{v}(t), \tag{2}$$

where $\mathbf{v}(t) \in \mathbb{R}^3$ is the vehicle velocity expressed in body-fixed coordinates. The kinematics of the velocity of the vehicle in body-fixed coordinates are modelled by

$$\dot{\mathbf{v}}(t) = \mathbf{a}(t) + \mathbf{g}(t) - \mathcal{S}(\omega(t))\,\mathbf{v}(t), \tag{3}$$

where $\mathbf{a}(t) \in \mathbb{R}^3$ is the accelerometer readings, $\mathbf{v}(t) \in \mathbb{R}^3$ is the velocity of the vehicle in body-fixed coordinates, and $\mathbf{g}(t) = \mathcal{R}^T(t)\,{}^I\mathbf{g}(t)$ is the body-fixed representation of the local gravity vector ${}^I\mathbf{g}(t) \in \mathbb{R}^3$, considered to be constant, that is, ${}^I\dot{\mathbf{g}}(t) = \mathbf{0}$. Thus, in body-fixed coordinates comes

$$\dot{\mathbf{g}}(t) = -\mathcal{S}(\omega(t))\,\mathbf{g}(t). \tag{4}$$

The distances between the transponder and the receivers installed on-board the vehicle (as measured by the USBL) can be written as

$$\rho_i(t) = \|\mathbf{b}_i - \mathbf{r}(t)\|, \quad i = 1, \ldots, n_r, \tag{5}$$

where $\mathbf{b}_i \in \mathbb{R}^3$ denotes the position of the i-th receiver in $\{B\}$, and n_r is the number of receivers of the USBL. Combining (2)-(5) yields the nonlinear system

$$\begin{cases} \dot{\mathbf{r}}(t) = -\mathcal{S}(\omega(t))\,\mathbf{r}(t) - \mathbf{v}(t), \\ \dot{\mathbf{v}}(t) = \mathbf{a}(t) + \mathbf{g}(t) - \mathcal{S}(\omega(t))\,\mathbf{v}(t), \\ \dot{\mathbf{g}}(t) = -\mathcal{S}(\omega(t))\,\mathbf{g}(t), \\ \rho_i(t) = \|\mathbf{b}_i - \mathbf{r}(t)\|,\ i = 1, \ldots, n_r. \end{cases} \tag{6}$$

The problem addressed in this paper is the following.

Problem statement 1. Consider a robotic vehicle that is equipped with an array of acoustic receivers that provide multiple range measurements to a fixed transponder in the mission operation scenario and an Inertial Measurement Unit (IMU), that consists of a triad of orthogonally mounted rate gyros and a triad of orthogonally mounted accelerometers, providing measurements of the vehicle angular velocity and linear acceleration. Design a filter or state observer for the transponder position $\mathbf{r}(t)$, the body-fixed vehicle velocity $\mathbf{v}(t)$, and the local gravity vector $\mathbf{g}(t)$ in body-fixed coordinates, considering noisy measurements for the vehicle angular velocity $\omega(t)$, the accelerometer readings $\mathbf{a}(t)$, and the ranges $\rho_i(t)$, with $i = 1, \ldots, n_r$.

3. FILTER DESIGN

In this section the main results and contributions of the paper are presented. In order to reduce the complexity of the system dynamics a Lyapunov state transformation is firstly introduced in Section 3.1. At the core of the proposed filtering framework is the derivation of a linear time-varying (LTV) system that captures the dynamics of the nonlinear system, which is proposed in Section 3.2, by means of an appropriate state augmentation. The nonlinear system dynamics are considered to their full extent and no linearizations are carried out whatsoever. The LTV model is shown to mimic the nonlinear system, and ultimately allows for the use of powerful linear system analysis and filtering design tools that yield a novel estimation solution with GAS error dynamics. The observability analysis of the LTV system and its relation with the original nonlinear system is conducted in Section 3.3, and finally in Section 3.4, the design of a Kalman filter is proposed in a stochastic setting for the resulting system. Although outside the scope of this work, the addition of an Attitude and Heading Reference System (AHRS) would allow for the final solution to be expressed directly in inertial coordinates.

3.1 State transformation

Consider the state transformation

$$\begin{bmatrix}\mathbf{x_1}(t)\\ \mathbf{x_2}(t)\\ \mathbf{x_3}(t)\end{bmatrix} := \mathbf{T}(t)\begin{bmatrix}\mathbf{r}(t)\\ \mathbf{v}(t)\\ \mathbf{g}(t)\end{bmatrix}, \tag{7}$$

where $\mathbf{T}(t) := \mathrm{diag}\left(\mathcal{R}(t), \mathcal{R}(t), \mathcal{R}(t)\right)$ is a Lyapunov state transformation which preserves all observability properties of the original system, see Brockett [1970].

The advantage of considering this state transformation is that the new unforced system dynamics becomes time-invariant, although the system output becomes time-varying and it is still nonlinear

$$\begin{cases}\dot{\mathbf{x}}_1(t) = -\mathbf{x_2}(t),\ \dot{\mathbf{x}}_2(t) = \mathbf{x_3}(t) + \mathbf{u}(t),\ \dot{\mathbf{x}}_3(t) = \mathbf{0},\\ \rho_i(t) = \|\mathbf{b}_i - \mathcal{R}^T(t)\mathbf{x_1}(t)\|,\ i = 1, \ldots, n_r,\end{cases} \tag{8}$$

where $\mathbf{u}(t) = \mathcal{R}(t)\mathbf{a}(t)$.

3.2 State augmentation

In order to derive a linear system that mimics the dynamics of the original nonlinear system, a state augmentation procedure follows inherited directly from the kinematics of the nonlinear range outputs of (8). Thus, taking the time-derivative of $\rho_i(t)$ in (8) yields

$$\dot{\rho}_i(t) = {}^1\!/_{\rho_i(t)}\left[{\mathbf{b}_i}^T\mathcal{S}\left(\omega(t)\right)\mathcal{R}^T(t)\mathbf{x_1}(t) + {\mathbf{b}_i}^T\mathcal{R}^T(t)\mathbf{x_2}(t) - {\mathbf{x_1}}^T(t)\mathbf{x_2}(t)\right]. \tag{9}$$

Identifying the nonlinear part ${\mathbf{x_1}}^T(t)\mathbf{x_2}(t)$ in (9) leads to the creation of the augmented states that will mimic this nonlinearity:

$$\begin{cases}x_{n_r+4}(t) = {\mathbf{x_1}}^T(t)\mathbf{x_2}(t),\\ x_{n_r+5}(t) = {\mathbf{x_1}}^T(t)\mathbf{x_3}(t) - \|\mathbf{x_2}(t)\|^2,\\ x_{n_r+6}(t) = {\mathbf{x_2}}^T(t)\mathbf{x_3}(t),\\ x_{n_r+7}(t) = \|\mathbf{x_3}(t)\|^2,\end{cases} \tag{10}$$

which correspond to the augmented dynamics

$$\begin{cases}\dot{x}_{n_r+4}(t) = \mathbf{u}^T(t)\mathbf{x_1}(t) + x_{n_r+5}(t),\\ \dot{x}_{n_r+5}(t) = -2\mathbf{u}^T(t)\mathbf{x_2}(t) - 3x_{n_r+6}(t),\\ \dot{x}_{n_r+4}(t) = \mathbf{u}^T(t)\mathbf{x_3}(t) + x_{n_r+7}(t),\\ \dot{x}_{n_r+7}(t) = \mathbf{0}.\end{cases} \tag{11}$$

Thus a new dynamic system is created by augmenting the original nonlinear system with the ranges corresponding states $x_4(t) := \rho_1(t)$, …, $x_{n_r+3}(t) := \rho_{n_r}(t)$, the augmented states defined in (10) and denoting the new augmented state vector $\mathbf{x}(t) \in \mathbb{R}^{13+n_r}$ by

$$\mathbf{x}(t) = \left[\,{\mathbf{x_1}}^T(t)\ {\mathbf{x_2}}^T(t)\ {\mathbf{x_3}}^T(t)\ x_4(t)\ \ldots\ x_{n_r+3}(t)\ x_{n_r+4}(t)\ \ldots x_{n_r+7}(t)\,\right]^T.$$

Combining the new augmented states dynamics with (8) it is easy to verify that the augmented dynamics can be written as

$$\dot{\mathbf{x}}(t) = \mathbf{A}(t)\mathbf{x}(t) + \mathbf{B}(t)\mathbf{u}(t),$$

where

$$\mathbf{A}(t) = \begin{bmatrix}
\mathbf{0} & -\mathbf{I} & \mathbf{0} & \mathbf{0} & 0 & 0 & 0 & 0\\
\mathbf{0} & \mathbf{0} & \mathbf{I} & \mathbf{0} & 0 & 0 & 0 & 0\\
\mathbf{0} & \mathbf{0} & \mathbf{0} & \mathbf{0} & 0 & 0 & 0 & 0\\
\frac{{\mathbf{b_1}}^T\mathcal{S}(\omega(t))\mathcal{R}^T(t)}{\rho_1(t)} & \frac{{\mathbf{b_1}}^T\mathcal{R}^T(t)}{\rho_1(t)} & \mathbf{0} & \mathbf{0} & -\frac{1}{\rho_1(t)} & 0 & 0 & 0\\
\vdots & \vdots & \vdots & \vdots & \vdots & \vdots & \vdots & \vdots\\
\frac{{\mathbf{b}_{n_r}}^T\mathcal{S}(\omega(t))\mathcal{R}^T(t)}{\rho_{n_r}(t)} & \frac{{\mathbf{b}_{n_r}}^T\mathcal{R}^T(t)}{\rho_{n_r}(t)} & \mathbf{0} & \mathbf{0} & -\frac{1}{\rho_{n_r}(t)} & 0 & 0 & 0\\
\mathbf{u}^T(t) & \mathbf{0} & \mathbf{0} & \mathbf{0} & 0 & 1 & 0 & 0\\
\mathbf{0} & -2\mathbf{u}^T(t) & \mathbf{0} & \mathbf{0} & 0 & 0 & -3 & 0\\
\mathbf{0} & \mathbf{0} & \mathbf{u}^T(t) & \mathbf{0} & 0 & 0 & 0 & 1\\
\mathbf{0} & \mathbf{0} & \mathbf{0} & \mathbf{0} & 0 & 0 & 0 & 0
\end{bmatrix}, \tag{12}$$

and

$$\mathbf{B}(t) = \left[\mathbf{0}_{3\times3}\ \mathbf{I}_3\ \mathbf{0}_{3\times3}\ \mathbf{0}_{3\times n_r}\ \mathbf{0}_{3\times4}\right]^T. \tag{13}$$

The following assumption is required so that (12) is well defined.

Assumption 2. The motion of the vehicle is such that

$$\exists_{\substack{R_{min}>0\\ R_{max}>0}}\ \forall_{\substack{t\geq t_0\\ i=1,\ldots,n_r}}\ :\ R_{min} \leq \rho_i(t) \leq R_{max}.$$

From a practical point of view this is not restrictive since the vehicle and the coupled array will never be on top of a transponder, and neither will the ranges converge to infinity. Moreover, the bounds R_{min} and R_{max} are not required for the filter synthesis in the sequel. Note that the RDOA at the receivers are considered to be measured more accurately compared to the absolute distance between the transponder and any given reference receiver of the USBL. Selecting a reference sensor on the array, for instance receiver 1 for now, all the other ranges are easily reconstructed from the range measured at receiver 1 and the RDOA between receiver 1 and the other receivers, that is $\rho_j(t) = \rho_1(t) - \delta\rho_{1j}(t)$, where $\delta\rho_{1j}(t) = \rho_1(t) - \rho_j(t)$, with $j \in \{2, \ldots, n_r\}$.

Taking into account that the augmented states $x_4(t), \ldots, x_{n_r+4}(t)$ that correspond to the ranges are actually measured, it is straightforward to show from the outputs of (6) that

$$\rho_i^2(t) - \rho_j^2(t) = \|\mathbf{b}_i\|^2 - \|\mathbf{b}_j\|^2 - 2(\mathbf{b}_i - \mathbf{b}_j)^T\mathcal{R}^T(t)\mathbf{x_1}(t),$$

with $i, j \in \{1, \ldots, n_r\}$, which leads to

$$\frac{2(\mathbf{b}_i - \mathbf{b}_j)^T\mathcal{R}^T(t)\mathbf{x_1}(t)}{\rho_i(t)+\rho_j(t)} + \rho_i(t) - \rho_j(t) = \frac{\|\mathbf{b}_i\|^2 - \|\mathbf{b}_j\|^2}{\rho_i(t)+\rho_j(t)}$$

or, equivalently

$$\frac{2(\mathbf{b}_i - \mathbf{b}_j)^T\mathcal{R}^T(t)\mathbf{x_1}(t)}{\rho_i(t)+\rho_j(t)} + x_{3+i}(t) - x_{3+j}(t) = \frac{\|\mathbf{b}_i\|^2 - \|\mathbf{b}_j\|^2}{\rho_i(t)+\rho_j(t)}, \tag{14}$$

where the right hand-side of (14) is measured and the left hand-side depends on the system state.

In order to complete the augmented system dynamics, discarding the original nonlinear outputs in (8), and considering (14), define the new augmented system outputs $\mathbf{y}(t) \in \mathbb{R}^{n_r+n_C}$ as

$$\mathbf{y}(t) = \begin{bmatrix}
\left[\,x_4(t)\ x_4(t) - x_5(t)\ \cdots\ x_4(t) - x_{3+n_r}(t)\,^T\right]\\
\frac{2(\mathbf{b_1}-\mathbf{b_2})^T\mathcal{R}^T(t)\mathbf{x_1}(t)}{\rho_1(t)+\rho_2(t)} + x_{3+1}(t) - x_{3+2}(t)\\
\frac{2(\mathbf{b_1}-\mathbf{b_3})^T\mathcal{R}^T(t)\mathbf{x_1}(t)}{\rho_1(t)+\rho_3(t)} + x_{3+1}(t) - x_{3+3}(t)\\
\vdots\\
\frac{2(\mathbf{b}_{n_r-1}-\mathbf{b}_{n_r})^T\mathcal{R}^T(t)\mathbf{x_1}(t)}{\rho_{n_r-1}(t)+\rho_{n_r}(t)} + x_{3+n_r-1}(t) - x_{3+n_r}(t)
\end{bmatrix},$$

where $n_C = C_2^{n_r} = {}^{n_r(n_r-1)}\!/_2$ is the number of all possible 2-combinations of n_r elements. Even though the observability analysis presented in the sequel does not require all possible combinations to bear constructive results (a subset of these combinations might yield the overall system observable), the derivation is presented using all n_C combinations in order to exploit all available information from the acoustic array in the filtering framework.

In compact form, the augmented system dynamics can be written as

$$\begin{cases}\dot{\mathbf{x}}(t) = \mathbf{A}(t)\mathbf{x}(t) + \mathbf{B}(t)\mathbf{u}(t),\\ \mathbf{y}(t) = \mathbf{C}(t)\mathbf{x}(t),\end{cases} \tag{15}$$

where

$$\mathbf{C}(t) = \begin{bmatrix}\mathbf{0}_{n_r\times3} & \mathbf{0}_{n_r\times6} & \mathbf{C_0} & \mathbf{0}_{n_r\times4}\\ \mathbf{C_1}(t)\mathcal{R}^T(t) & \mathbf{0}_{n_C\times6} & \mathbf{C_2} & \mathbf{0}_{n_C\times4}\end{bmatrix},$$

$$\mathbf{C_0} = \begin{bmatrix} 1 & 0 & \cdots & 0 \\ 1 & -1 & & \\ \vdots & & \ddots & \\ \vdots & \mathbf{0} & & \mathbf{0} \\ 1 & & & -1 \end{bmatrix}, \quad \mathbf{C_2} = \begin{bmatrix} 1 & -1 & 0 & 0 & \cdots & 0 \\ 1 & 0 & -1 & 0 & \cdots & 0 \\ & & & \vdots & & \\ 0 & \cdots & 0 & 1 & 0 & -1 \\ 0 & \cdots & 0 & 0 & 1 & -1 \end{bmatrix},$$

and

$$\mathbf{C_1}(t) = 2 \begin{bmatrix} \frac{(\mathbf{b}_1 - \mathbf{b}_2)}{\rho_1(t)+\rho_2(t)} & \frac{(\mathbf{b}_1 - \mathbf{b}_3)}{\rho_1(t)+\rho_3(t)} & \cdots & \frac{(\mathbf{b}_{n_r-1} - \mathbf{b}_{n_r})}{\rho_{n_r-1}(t)+\rho_{n_r}(t)} \end{bmatrix}^T. \quad (16)$$

3.3 Observability analysis

The Lyapunov state transformation and the state augmentation that were carried out allowed to derive the LTV system described in (15), which ensembles the behavior of the original nonlinear system (6). The dynamic system (15) can be regarded as LTV, even though the system matrix $\mathbf{A}(t)$ depends explicitly on the system input and output, as evidenced by (12). Nevertheless, this is not a problem from the theoretical point of view since both the input and output of the system are known continuous bounded signals. The idea is not new either, see, e.g., Celikovsky and Chen [2005], and it just suggests, in this case, that the observability of (15) may be connected with the evolution of the system input or output (or both), which is not common and does not happen when this matrix does not depend on the system input or output.

In order to fully understand and couple the behavior of both systems, the observability analysis of (15) is carried out in this section, using classical theory of linear systems. This analysis is conducted based on the observability Gramian associated with the pair $(\mathbf{A}(t), \mathbf{C}(t))$, which is given by (see Antsaklis and Michel [2006])

$$\mathcal{W}(t_0, t_f) = \int_{t_0}^{t_f} \Phi^T(t, t_0)\mathbf{C}^T(t)\mathbf{C}(t)\Phi(t, t_0)dt,$$

where $\Phi(t, t_0)$ is the state transition matrix of the LTV system (15).

Before proceeding with the observability analysis, the following assumption is introduced which ultimately asserts the minimal number of receivers and configuration requirements of the USBL array in order to render the system observable regardless of the trajectory described of the vehicle.

Assumption 3. There are at least 4 non-coplanar receivers.

The reasoning behind the need to have at least 4 non-coplanar receivers is that this is the minimal configuration that guarantees the uniqueness for the transponder position $\mathbf{r}(t)$. The following theorem establishes the observability of the LTV system (15).

Theorem 4. The linear time-varying system (15) is observable on $[t_0, t_f]$, $t_0 < t_f$.

Proof. The proof follows by establishing that the only solution of

$$\mathbf{d}^T\mathcal{W}(t_0, t_f)\mathbf{d} = 0$$

is $\mathbf{d} = \mathbf{0}$, which means that the system is observable. It is omitted due to the lack of space.

Although the observability of the LTV system (15) has been established, it does not mean that the original nonlinear system (6) is also observable, and neither means that an observer for (15) is also an observer for (6). This however turns out to be true, as it is shown in the next theorem.

Theorem 5. The nonlinear system (8) is observable in the sense that, given $\{\mathbf{y}(t), t \in [t_0, t_f]$ and $\{\mathbf{u}(t), t \in [t_0, t_f]$, the initial state $\mathbf{x}(t_0) = \left[\mathbf{x}_1{}^T(t_0)\ \mathbf{x}_2{}^T(t_0)\ \mathbf{x}_3{}^T(t_0) \right]^T$ is uniquely defined. Moreover, a state observer for the LTV system (15) with globally asymptotically stable error dynamics is also a state observer for the nonlinear system (8), with globally asymptotically stable error dynamics.

Proof. The observability of the LTV system (15) has already been established in Theorem 4, thus given $\{\mathbf{y}(t), t \in [t_0, t_f]\}$ and $\{\mathbf{u}(t), t \in [t_0, t_f]\}$, the initial state of (15) is uniquely defined. Let $\mathbf{z}(t_0) \in \mathbb{R}^{13+n_r}$ be the initial state of the LTV system (15) and $\mathbf{x}(t_0) \in \mathbb{R}^9$ be the initial state of the nonlinear system (8). The proof is accomplished by comparing the difference of the squared ranges $\rho_i^2(t) - \rho_j^2(t)$ for both systems, and concluding that given $\{\mathbf{y}(t), t \in [t_0, t_f]\}$ and $\{\mathbf{u}(t), t \in [t_0, t_f]\}$, the initial states in $\mathbf{x}(t_0)$ must match the corresponding initial states in $\mathbf{z}(t_0)$, which are uniquely defined, and therefore concludes the proof. □

Note that the usual concept of observability for nonlinear systems is not as strong as that presented in the statement of Theorem 5, see Hermann and Krener [1977]. Although the observability results were derived with respect to the nonlinear system (8), they also apply to the original nonlinear system (6) as they are related through a Lyapunov transformation. Thus, the design of a filter for the original nonlinear system follows simply by reversing the state transformation (7), as it will be detailed in the following section.

3.4 Kalman filter

The observer structure devised so far was based on a deterministic setting providing strong constructive results, in the sense that it was shown, in Theorem 5, that an observer with globally asymptotically stable error dynamics for the LTV system (15) provides globally asymptotically stable error dynamics for the estimation of the state of the original nonlinear system. However, in practice there exists measurement noise and system disturbances, motivating the derivation of a filtering solution within a stochastic setting. Therefore, the design of a LTV Kalman Filter (even tough other filtering solutions could be used, e.g. a $\mathcal{H}_\infty$ filter) is presented next. Before proceeding with the derivation of the proposed filter, it is important to stress, however, that this filter is not optimal, as the existence of multiplicative noise is evident by looking into the LTV system matrices.

Nevertheless, the errors associated with the Kalman filter estimates are GAS, as it can be shown that the system is not only observable but also uniformly completely observable, a sufficient condition for the stability of the LTV Kalman filter, see Anderson [1971]. The following assumption is introduced to guarantee the uniform complete observability of the system.

Assumption 6. The position of the transponder in the vehicle coordinate frame $\mathbf{r}(t)$, the angular and linear velocities, $\omega(t)$ and $\mathbf{v}(t)$ respectively, and the specific force that acts on the vehicle $\mathbf{a}(t)$, are bounded signals. Moreover, the time derivatives of these signals ($\dot{\mathbf{r}}(t)$, $\dot{\omega}(t)$, $\dot{\mathbf{v}}(t)$, $\dot{\mathbf{a}}(t)$ respectively), are also bounded, as well as the derivatives of the ranges $\dot{\rho}_i(t)$, with $i = 1, \ldots, n_r$.

From a practical point of view, Assumption 6 is not restrictive since the systems presented herein are in fact finite energy systems that ensemble realizable physical vehicles and sensors. The LTV system (15) is finally shown to be uniformly completely observable in the following theorem.

Theorem 7. The linear time-varying system (15) is uniformly completely observable, that is, there exists positive constants α_1, α_2, δ, such that $\alpha_1\mathbf{I} \preceq \mathcal{W}(t, t+\delta) \preceq \alpha_2\mathbf{I}$ for all $t \geq t_0$.

Proof. The proof starts by noticing that the bounds on the observability Gramian $\mathcal{W}(t, t+\delta)$ can be written as $\alpha_1 \leq \int_t^{t+\delta} \|\mathbf{C}(\tau)\mathbf{\Phi}(\tau, t)\mathbf{d}\|^2 d\tau \leq \alpha_2$, for all $t \geq t_0$, and for all $\mathbf{d} \in \mathbb{R}^{13+n_r}$ such that $\|\mathbf{d}\| = 1$. The existence of the upper bound α_2 is trivially checked, as under Assumption 6 the matrices $\mathbf{A}(t)$ and $\mathbf{C}(t)$ are norm-bounded and $\|\mathbf{C}(\tau)\mathbf{\Phi}(\tau, t)\mathbf{d}\|^2$ is integrated over limited intervals. By selectively setting non-null parts of $\mathbf{d}$, the lower bound α_1 can be shown to exist for every possible $\mathbf{d} \in \mathbb{R}^{13+n_r}$ such that $\|\mathbf{d}\| = 1$. □

To recover the augmented system dynamics in the original coordinate space, the original Lyapunov state transformation (7) is reverted considering the augmented state transformation $\mathbf{\Gamma}(t) := \mathbf{T_r}(t)\mathbf{x}(t)$, where $\mathbf{T_r}(t) := \text{diag}\left(\mathcal{R}^T(t), \mathcal{R}^T(t), \mathcal{R}^T(t), 1, \ldots, 1\right)$ is a also Lyapunov state transformation that preserves all observability properties of the LTV system (15).

Including system disturbances and sensor noise yields the final augmented dynamics

$$\begin{cases} \dot{\mathbf{\Gamma}}(t) = \mathbf{A_\Gamma}(t)\mathbf{\Gamma}(t) + \mathbf{B_\Gamma}(t)\mathbf{v_r}(t) + \mathbf{n_x}(t), \\ \mathbf{y}(t) = \mathbf{C_\Gamma}(t)\mathbf{\Gamma}(t) + \mathbf{n_y}(t), \end{cases}$$

where

$$\mathbf{A_\Gamma}(t) = \begin{bmatrix} -\mathcal{S}(\omega(t)) & -\mathbf{I} & \mathbf{0} & \mathbf{0}_{3\times n_r} & 0 & 0 & 0 & 0 \\ \mathbf{0} & -\mathcal{S}(\omega(t)) & \mathbf{I} & \mathbf{0}_{3\times n_r} & 0 & 0 & 0 & 0 \\ \mathbf{0} & \mathbf{0} & -\mathcal{S}(\omega(t)) & \mathbf{0}_{3\times n_r} & 0 & 0 & 0 & 0 \\ \frac{\mathbf{b}_1{}^T\mathcal{S}(\omega(t))}{\rho_1(t)} & \frac{\mathbf{b}_1{}^T}{\rho_1(t)} & \mathbf{0} & \mathbf{0}_{1\times n_r} & -\frac{1}{\rho_1(t)} & 0 & 0 & 0 \\ \vdots & \vdots & \vdots & \vdots & \vdots & & & \\ \frac{\mathbf{b}_{n_r}{}^T\mathcal{S}(\omega(t))}{\rho_{n_r}(t)} & \frac{\mathbf{b}_{n_r}{}^T}{\rho_{n_r}(t)} & \mathbf{0} & \mathbf{0}_{1\times n_r} & -\frac{1}{\rho_{n_r}(t)} & 0 & 0 & 0 \\ \mathbf{u}^T(t) & \mathbf{0} & \mathbf{0} & \mathbf{0}_{1\times n_r} & 0 & 1 & 0 & 0 \\ \mathbf{0} & -2\mathbf{u}^T(t) & \mathbf{0} & \mathbf{0}_{1\times n_r} & 0 & 0 & -3 & 0 \\ \mathbf{0} & \mathbf{0} & \mathbf{u}^T(t) & \mathbf{0}_{1\times n_r} & 0 & 0 & 0 & 1 \\ \mathbf{0} & \mathbf{0} & \mathbf{0} & \mathbf{0}_{1\times n_r} & 0 & 0 & 0 & 0 \end{bmatrix},$$

$$\mathbf{C_\Gamma}(t) = \begin{bmatrix} \mathbf{0}_{n_r\times 3} & \mathbf{0}_{n_r\times 6} & \mathbf{C_0} & \mathbf{0}_{n_r\times 4} \\ \mathbf{C_1}(t) & \mathbf{0}_{n_C\times 6} & \mathbf{C_2} & \mathbf{0}_{n_C\times 4} \end{bmatrix},$$

where $\mathbf{B_\Gamma}(t) = \mathbf{B}(t)$ is defined in (13), $\mathbf{C_1}(t)$ is defined in (16), and $\mathbf{n_x}(t)$ and $\mathbf{n_y}(t)$ are assumed to be uncorrelated, zero-mean, white Gaussian noise, with $E\left[\mathbf{n_x}(t)\mathbf{n_x}{}^T(\tau)\right] = \mathbf{Q_x}(t)\delta(t-\tau)$ and $E\left[\mathbf{n_y}(t)\mathbf{n_y}{}^T(\tau)\right] = \mathbf{Q_y}(t)\delta(t-\tau)$.

4. SIMULATION RESULTS

The performance of the proposed filter was assessed in simulation using a kinematic model for an underwater vehicle. The vehicle describes a typical survey trajectory followed by a dive and approach towards the transponder, as depicted in Fig. 2.

The USBL receiving array is composed of 4 receivers that are installed on the vehicle with an offset of 30 cm along

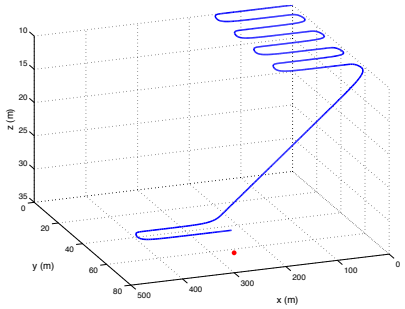

Fig. 2. Vehicle nominal trajectory (in blue) and transponder position (in red)

the x-axis of the body-fixed coordinate frame $\{B\}$ where the IMU is also installed in a strap-down configuration. Thus the positions of the receivers with respect $\{B\}$ are given in meters by $\mathbf{b}_1 = [0.2\ -0.15\ 0]^T$, $\mathbf{b}_2 = [0.2\ 0.15\ 0]^T$, $\mathbf{b}_3 = [0.4\ 0\ 0.15]^T$, and $\mathbf{b}_4 = [0.4\ 0\ -0.15]^T$ $[m]$.

The triad of accelerometers is inspired on a realistic commercially available sensor package, the Crossbow CXL10TG3 triaxial accelerometer, and considered to provide specific force measurements corrupted by additive uncorrelated, zero-mean white Gaussian noise, with a standard deviation of 0.6 mg, that is, 5.886×10^{-3} $[m/s^2]$ for a gravity constant $g \approx 9.81$ $[m/s^2]$. The rate gyros are also inspired on a realistic sensor package, the Silicon Sensing CRS03 triaxial rate gyro, and are thus considered to be disturbed by additive, uncorrelated, zero-mean white Gaussian noise, with a standard deviation of 0.05 deg/s.

The range measurements between the transponder and the reference receiver (receiver 1) are considered to be disturbed by additive, zero-mean white Gaussian noise, with a standard deviation equivalent to 0.2% of the slant-range, whilst the RDOA between receiver 1 and the other 3 receivers is considered to be measured with an accuracy of 6 mm. The transponder is located in inertial coordinates at ${}^I\mathbf{p}_t = [300\ 80\ 32]^T$ $[m]$. The augmented states that correspond to the ranges $x_4, \ldots, x_{3+n_r}$ are initialized with the first set of measurements available, and the augmented state estimate that corresponds to the squared norm of the local gravity vector is initialized to $x_{n_r+7} = 100$, an approximate value of the squared gravity constant. The filter position estimate is initialized with an offset of 20 m from the nominal position, the local gravity vector is initialized to $\mathbf{x}_3(t_0) = [0\ 0\ 10]^T$, and the remaining initial estimates are set to zero.

The output estimation error of the proposed filter is depicted in Figure 3, where the fast initial convergence of the estimates is evident. The augmented states of the LTV Kalman Filter also exhibit a fast convergence, evidenced in Fig. 4. The steady state response of the filter is also compared to the classical Extended Kalman Filter (EKF) that linearizes the nonlinear range and RDOA measurements about the filter estimates in order to compute a suboptimal Kalman gain, and it is shown to attain the same performance level as this traditional filtering solution. Although omitted due to the lack of space, simulation results also evidenced that the proposed filtering structure outperforms more classical solutions based on the Planar-Wave approximation, in which the feedback is accomplished by means of a precomputed transponder position fix from the USBL that resorts

to a planar-wave approximation, previously used by the authors in Morgado et al. [2006a]. The solution presented in this work has the advantage of being GAS, which is not guaranteed for the other designs.

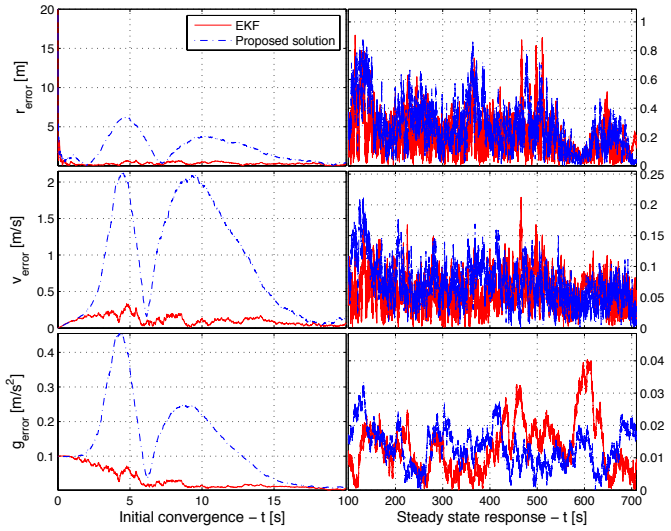

Fig. 3. LTV Kalman filter error evaluation and comparison with EKF - Initial convergence and steady state

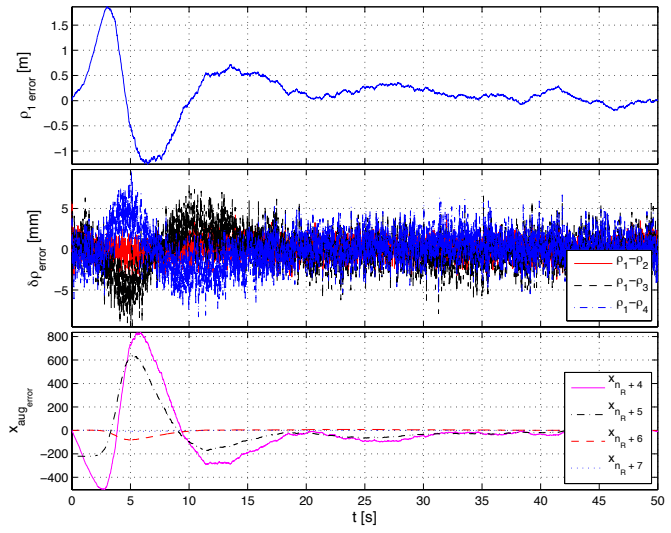

Fig. 4. LTV Kalman filter augmented states initial convergence

5. CONCLUSIONS

The main contribution of the paper lies on the design of globally asymptotically stable position filters based directly on the nonlinear sensor readings of an USBL acoustic positioning sensor and an IMU. At the core of the proposed filtering solution is the derivation of a LTV system that fully captures the dynamics of the nonlinear system. The LTV model is achieved through appropriate state augmentation allowing for the use of powerful linear system analysis and filtering design tools that yield GAS filter error dynamics. The implementation of the proposed filtering solution in real-life hardware will require a discrete setup that is able to cope with the different update rates of the various sensors installed on-board, and will be addressed in future developments of this work. Nonetheless, the proposed continuous-time framework allowed for the development of strong constructive results in terms of global asymptotic error stability.

The performance of the proposed filter was assessed in simulation and compared against a more traditional solution based on the Extended Kalman Filter (EKF). Numerical simulation results allowed to conclude that the proposed filter is able to achieve the same performance level of the EKF using realistic sensor noise and disturbances. Future work will also include further evaluation of the system performance and comparison with traditional solutions, through extensive Monte-Carlo numerical simulations and with experimental results. The advantage of the new filter structure is nevertheless evident, due to its GAS properties which is not guaranteed for the traditional solution.

REFERENCES

B. Anderson. Stability properties of Kalman-Bucy filters. *Journal of the Franklin Institute*, 291(2):137–144, 1971.

P.J. Antsaklis and A.N. Michel. *Linear systems*. Birkhauser, 2006.

P. Batista, C. Silvestre, and P. Oliveira. Single Range Navigation in the presence of Constant Unknown Drifts. In *Proceedings of the European Control Conference 2009 - ECC'09*, Budapest, Hungary, August 2009.

P. Batista, C. Silvestre, and P. Oliveira. Optimal position and velocity navigation filters for autonomous vehicles. *Automatica*, 46(4):767–774, April 2010.

R. W. Brockett. *Finite Dimensional Linear Systems*. Wiley, 1970.

S. Celikovsky and G. Chen. Secure synchronization of a class of chaotic systems from a nonlinear observer approach. *IEEE Transactions on Automatic Control*, 50(1):76–82, 2005.

R. Hermann and A. J. Krener. Nonlinear controllability and observability. *IEEE Transactions on Automatic Control*, 22(5):728–740, 1977.

M. Morgado, P. Oliveira, C. Silvestre, and J.F. Vasconcelos. USBL/INS Tightly-Coupled Integration Technique for Underwater Vehicles. In *Proceedings Of The 9th International Conference on Information Fusion*, Florence, Italy, July 2006a. IEEE.

M. Morgado, P. Oliveira, C. Silvestre, and J.F. Vasconcelos. USBL/INS Integration Technique for Underwater Vehicles. In *Proceedings Of The 7th IFAC Conference on Manoeuvring and Control of Marine Craft*, Lisbon, Portugal, September 2006b. IFAC.

M. Morgado, P. Batista, C. Silvestre, and P. Oliveira. Position USBL/DVL Sensor-based Navigation Filter in the presence of Unknown Ocean Currents. In *The Proceedings of the IEEE 49th Conference on Decision and Control*, Atlanta, GA, USA, 2010.

P. Rigby, O. Pizarro, and S.B. Williams. Towards Geo-Referenced AUV Navigation Through Fusion of USBL and DVL Measurements. In *OCEANS 2006*, Sept. 2006.

L. L. Whitcomb. Underwater robotics: out of the research laboratory and into the field. In *Robotics and Automation, 2000. Proceedings. ICRA '00. IEEE International Conference on*, volume 1, pages 709–716 vol.1, 2000.

E. Willemenot, P.-Y. Morvan, H. Pelletier, and A. Hoof. Subsea positioning by merging inertial and acoustic technologies. In *OCEANS 2009-EUROPE, 2009. OCEANS '09.*, pages 1–8, May 2009.